

High *Skp2* Expression Characterizes High-Risk Neuroblastomas Independent of *MYCN* Status

Frank Westermann,¹ Kai-Oliver Henrich,¹ Jun S. Wei,² Werner Lutz,³ Matthias Fischer,⁴ Rainer König,^{5,6} Ruprecht Wiedemeyer,¹ Volker Ehemann,⁷ Benedikt Brors,⁵ Karen Ernestus,⁴ Ivo Leuschner,⁹ Axel Benner,⁸ Javed Khan,² and Manfred Schwab¹

Abstract Purpose: Amplified *MYCN* oncogene defines a subgroup of neuroblastomas with poor outcome. However, a substantial number of *MYCN* single-copy neuroblastomas exhibits an aggressive phenotype similar to that of *MYCN*-amplified neuroblastomas even in the absence of high *MYCN* mRNA and/or protein levels.

Experimental Design: To identify shared molecular mechanisms that mediate the aggressive phenotype in *MYCN*-amplified and single-copy high-risk neuroblastomas, we defined genetic programs evoked by ectopically expressed *MYCN in vitro* and analyzed them in high-risk versus low-risk neuroblastoma tumors ($n = 49$) using cDNA microarrays. Candidate gene expression was validated in a separate cohort of 117 patients using quantitative PCR, and protein expression was analyzed in neuroblastoma tumors by immunoblotting and immunohistochemistry.

Results: We identified a genetic signature characterized by a subset of *MYCN/MYC* and *E2F* targets, including *Skp2*, encoding the F-box protein of the SCF^{Skp2} E3-ligase, to be highly expressed in high-risk neuroblastomas independent of amplified *MYCN*. We validated the findings for *Skp2* and analyzed its expression in relation to *MYCN* and *E2F-1* expression in a separate cohort ($n = 117$) using quantitative PCR. High *Skp2* expression proved to be a highly significant marker of dire prognosis independent of both *MYCN* status and disease stage, on the basis of multivariate analysis of event-free survival (hazard ratio, 3.54; 95% confidence interval, 1.56-8.00; $P = 0.002$). *Skp2* protein expression was inversely correlated with expression of p27, the primary target of the SCF^{Skp2} E3-ligase, in neuroblastoma tumors.

Conclusion: *Skp2* may have a key role in the progression of neuroblastomas and should make an attractive target for therapeutic approaches.

The embryonal tumor neuroblastoma is the most common solid extracranial tumor in young children and is derived from primitive cells of the sympathetic nervous system. The biological behavior of neuroblastomas is extremely variable.

In many patients, neuroblastoma is metastatic at the time of diagnosis and usually undergoes rapid progression with fatal outcome. Neuroblastomas tend to regress spontaneously in a portion of infants younger than age 1 year at diagnosis or to differentiate into benign ganglioneuroma in some older patients (1, 2). Deregulated *MYCN* is thought to play an important role in tumor progression; amplified *MYCN* oncogene is strongly associated with advanced-stage disease and poor outcome (3). The oncogenic properties of *MYCN* overexpression have been shown in various experimental systems *in vitro* and *in vivo* (4, 5). However, a considerable number of *MYCN* single-copy neuroblastomas exhibits an aggressive phenotype similar to that of *MYCN*-amplified tumors even in the absence of high *MYCN* mRNA and/or protein levels (6, 7), suggesting other unfavorable molecular abnormalities that could account for the inferior survival.

Recently, DNA microarray technology has been applied to study gene expression profiles in primary neuroblastomas. Patterns of differentially expressed genes among different neuroblastoma subtypes as well as gene expression classifiers have emerged, allowing a better prediction of patient's outcome than established risk markers (8-12). A consistent finding from these studies was that a subset of cell cycle genes are expressed at higher levels in high-risk neuroblastomas independent of the genomic *MYCN* status. In general, it is

Authors' Affiliations: ¹Department of Tumor Genetics, German Cancer Research Center, Heidelberg, Germany; ²Oncogenomics Section, Pediatric Oncology Branch, Advanced Technology Center, National Cancer Institute, Gaithersburg, Maryland; ³Institute of Molecular Biology and Tumor Research, University of Marburg, Marburg, Germany; ⁴Department of Pediatric Oncology, University Children's Hospital of Cologne, Cologne, Germany; ⁵Theoretical Bioinformatics, German Cancer Research Center; ⁶Department of Bioinformatics and Functional Genomics, Institute of Pharmacy and Molecular Biotechnology and ⁷Department of Pathology, University of Heidelberg; ⁸Department of Biostatistics, German Cancer Research Center, Heidelberg, Germany; and ⁹Department of Pathology, University of Kiel, Kiel, Germany Received 11/28/06; revised 4/7/07; accepted 5/29/07.

Grant support: Krebshilfe, BMBF (NGFN2), Deutsche Forschungsgemeinschaft, and the European Union.

The costs of publication of this article were defrayed in part by the payment of page charges. This article must therefore be hereby marked *advertisement* in accordance with 18 U.S.C. Section 1734 solely to indicate this fact.

Note: Supplementary data for this article are available at Clinical Cancer Research Online (<http://clincancerres.aacrjournals.org/>).

Requests for reprints: Frank Westermann, Department of Tumour Genetics, German Cancer Research Center, Im Neuenheimer Feld 280, Heidelberg, BW 69221, Germany. Phone: 49-622-1423275; E-mail: f.westermann@dkfz.de.

© 2007 American Association for Cancer Research.
doi:10.1158/1078-0432.CCR-06-2818

believed that elevated expression of cell cycle genes reflects higher proliferation rates of tumor cells from more aggressive subtypes. Elevated expression of cell cycle genes, which are largely regulated by E2F transcription factors, also implies an impaired Rb pathway that fails to control E2F activity. It has been reported that high *E2F-1*, an E2F member but also a prototypical E2F target gene, is universally found in high-risk neuroblastomas independent of genomic *MYCN* status (13). Although it is known that *MYCN* increases E2F activity and cell cycle progression, the precise molecular mechanisms by which *MYCN* favors G₁-S phase transition are poorly understood. Due to the absence of high *MYCN* levels in *MYCN* single-copy high-risk neuroblastomas, it is also not clear whether activation of *MYCN*-regulated genes plays a significant role in uncontrolled cell cycle progression in this neuroblastoma subtype.

Gene expression profiling of artificial *in vitro* systems allowing the ectopic expression of oncoproteins have been successfully used to characterize and predict the activity of oncogenic pathways in *in vivo* tumor models (14). In this study, we sought to define genetic programs evoked by ectopically expressed *MYCN* *in vitro*. We hypothesized that by analyzing the activity of these *MYCN*-related genetic programs in relation to patients' outcome, it should be possible to identify components downstream of *MYCN* that are involved in neuroblastoma tumor progression independent of genomic *MYCN* status. Using cDNA microarray analysis of neuroblastoma cells after conditional expression of *MYCN* *in vitro* and of 49 primary neuroblastoma tumors, we identified a subset of direct *MYCN*/*MYC* and E2F targets that provided information on patients' outcome additionally to genomic *MYCN* status or *MYCN* expression. As an alternative mechanism that enhances *MYCN* target gene activation in *MYCN* single-copy neuroblastoma tumors, we considered the deregulated activity of a cofactor involved in transcriptional activation by *MYC* proteins. We found *Skp2*, encoding the F-box protein of the SCF^{Skp2} ubiquitin ligase that is required for the transcriptional activation of *MYC* target genes (15), highly coexpressed with *MYCN*/*MYC* and E2F target genes in high-risk neuroblastoma

tumors. We analyzed the expression of *Skp2* in relation to *MYCN* and *E2F-1* in a separate cohort of 117 neuroblastoma patients using quantitative PCR (QPCR). Because *Skp2* also favors G₁-S (16, 17) as well as G₂-M transition (18) via the degradation of cell cycle regulatory proteins, such as p27 and p21, we investigated the relation of *Skp2* and p27 protein levels in neuroblastoma specimens using immunoblotting and immunohistochemistry.

Materials and Methods

Patients. All patients were enrolled in the German Neuroblastoma Trial and diagnosed between 1991 and 2002. The cohort available for cDNA microarray analysis consisted of 49 patients and for QPCR analysis of 117 patients (Table 1). Tumor samples were collected before any cytoreductive treatment. The only criterion for patient selection was availability of sufficient amounts of tumor material. The composition of the cohorts in terms of tumor stage, *MYCN* status, and age at diagnosis was in agreement with the composition of an unselected cohort of 1,741 patients diagnosed between 1990 and 2003 in Germany (ref. 19; data not shown). Standard prognostic markers were assessed in the reference laboratories of the German neuroblastoma trial in Köln, Marburg, Heidelberg, Stuttgart, and Zürich. Informed consent was obtained from patients' parents. Patients were treated according to the guidelines established by the German Neuroblastoma Trial, with risk stratification criteria as described elsewhere (20). All samples had a minimal tumor cell content of 65%, as determined by histologic examination.

Microarray experiments. Microarray experiments were done as described previously (10). The reference RNA used in the study for tumor specimens consisted of equal portions of total RNA obtained from seven human cancer cell lines (10). The microarrays used in the studies consisted of 42,578 cDNA clones, representing 25,933 UniGene clusters. Hybridization and washing of the microarrays were done as described (10). The raw data of both tumor samples and cell line experiments were normalized with the variance normalization method (21) as implemented in the R VSN package.¹⁰ The SH-EP-*MYCN* cell line expressing a *MYCN* transgene under the control of a tetracycline-repressible element (22) was used to generate gene expression profiles after targeted *MYCN* expression. Total RNA was collected from SH-EP-*MYCN* cells after targeted *MYCN* expression at different experimental conditions to better distinguish between direct *MYCN* and E2F targets (refs. 22, 23; see also Supplementary Data and Methods). The microarray data are available online (accession nos. E-CVDE-2 and E-CVDE-3).¹¹

Quantitative real-time reverse transcription-PCR. First-strand cDNA was generated from total RNA using the Superscript II First-Strand Synthesis System (Invitrogen) according to the manufacturer's directions. QPCR was done on an ABI PRISM 7700 Sequence Detection System (Applied Biosystems) with SYBR Green chemistry using the standard curve method (user bulletin no. 2, ABI PRISM 7700 SDS). For normalization, the expression level of the target genes was divided by the geometric mean of expression levels of the housekeeping genes *hypoxanthine phosphoribosyltransferase 1* (*HPRT1*) and *succinate dehydrogenase complex, subunit A* (*SDHA*), as described previously (24, 25). The geometric mean of *HPRT1* and *SDHA* transcript levels was shown to represent a low variability internal control for investigating differential gene expression in primary neuroblastoma by QPCR (24). Primer sequences were as follows: 5'-TCCGGAGAGGACACCCCTG-3' (*MYCN*-forward), 5'-GCCTTGGTGTGGAGGAGG-3' (*MYCN*-reverse), 5'-TACAGAAAGAATCTCCAGAAATCAGATC-3' (*Skp2*-forward), 5'-GGAAAAATTCCGTAAAGCAGTCA-3' (*Skp2*-reverse), 5'-AGCGGCGCATCTATGACATC-3'

Table 1. Patient characteristics

	Microarray cohort, n (%)	QPCR cohort, n (%)
INSS		
1	14 (29)	19 (16)
2	4 (8)	9 (8)
3	8 (16)	15 (13)
4	17 (35)	48 (41)
4s	6 (12)	26 (22)
Amplified <i>MYCN</i>		
No	38 (78)	101 (86)
Yes	11 (22)	16 (14)
Age at diagnosis (y)		
<1.5	33 (67)	71 (61)
>1.5	16 (33)	46 (39)
Total	49	117

NOTE: Microarray cohort and QPCR cohort overlapped by 17 tumors. Thus, 149 tumors were investigated in total.
Abbreviation: INSS, International Neuroblastoma Staging System.

¹⁰ www.r-project.org

¹¹ http://www.ebi.ac.uk/miamexpress/

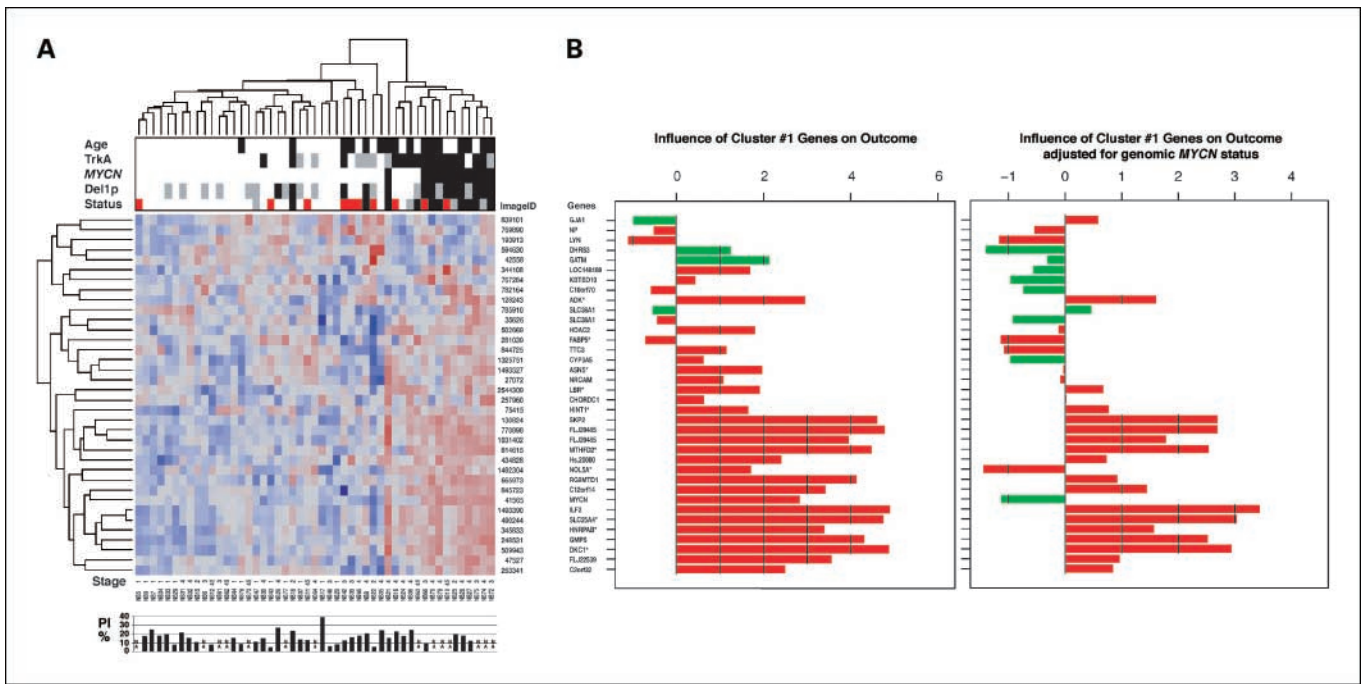


Fig. 1. Association of *MYCN in vitro* clusters 1 and 176 with clinical outcome in neuroblastoma tumors. Two-way hierarchical cluster analysis using cluster 1 (A) and cluster 176 (C) genes together with two gene plots (B and D) from the Global Test for each cluster. The two gene plots illustrate the influence on overall survival of each gene from clusters 1 (A), representing a typical group A cluster (enriched with *MYCN/MYC* target genes, verified targets are marked with *), and 176 (B), representing a group B cluster (enriched with *E2F* target genes). The gene plot gives the influence on overall survival without (left) and with (right) adjustment for the variable genomic *MYCN* status. The gene plot shows a bar and a reference line for each gene tested. In a survival model, the expected height is zero under the null hypothesis that the gene is not associated with the clinical outcome (= reference line). Marks in the bars indicate with how many SDs the bar exceeds the reference line. The bars are colored to indicate a positive (green) or a negative (red) association of the gene expression with survival. Tumor cell proliferation indices (*PI*; % S phase + % G₂-M phase) were calculated from cell cycle profiles as determined by fluorescence-activated cell sorting analysis. Data on proliferation indices were not available for all tumors (NA). Clinical variables (age at diagnosis, white, 1.5 y; black, ≥ 1.5 y; tumor stage at diagnosis; status, white, alive at least 3 y after diagnosis; red, relapse/progression; black, death due to neuroblastoma; gray, death due to other causes) and molecular markers (TrkA protein expression, white, high; black, low; gray, not available; genomic *MYCN* status, white, single-copy; black, amplified; chromosome 1p status, white, normal; black, 1p deleted; gray, not available) are added to the heat map of gene expression.

(*E2F-1*-forward), 5'-TCAACCCCTCAAGCCGTC-3' (*E2F-1*-reverse), 5'-TGGAACAAGAGGGCATCTG-3' (*SDHA*-forward), 5'-CCACCACTGCATCAAATTCATG-3' (*SDHA*-reverse), 5'-TGACACTGGCAAACAATGCA-3' (*HPRT1*-forward), and 5'-GGTCCTTTTACCAGCAAGCT-3' (*HPRT1*-reverse).

Flow cytometric analysis. Native or snap-frozen human neuroblastoma tumor tissues as well as single cells from cell culture experiments were monitored for DNA indices and cell cycle distribution by flow cytometry (fluorescence-activated cell sorting) as described (26). Each histogram represents 30,000 to 100,000 cells for measuring DNA index and cell cycle. Histogram analysis was done with the Multicycle program (Phoenix Flow Systems). Human lymphocyte nuclei from healthy donors were used as internal standard for determination of the diploid cell population. The mean coefficient of variation of diploid lymphocytes was 0.8 to 1.0.

Protein analysis. Protein expression was assessed by immunoblotting using 50 μ g of total cell lysates from tumor sections as previously described (27). Blots were probed with antibodies directed against p27 (Dako), Skp2 (Zymed), *E2F-1* (BD Bioscience), and β -actin (Sigma) as loading control. Immunohistochemistry was done using the same antibodies on a paraffin multitissue array containing 141 neuroblastomas and evaluated by a pathologist (K.E.). For p27 immunostaining, a biotin-avidin method was applied, as described earlier (28). The sections were boiled in EDTA buffer (pH 9.0) for 20 min and then incubated with the primary antibody p27 at a dilution of 1:25 for 30 min at room temperature. For Skp2 immunostaining, an enhanced biotin-avidin method was used, as described earlier (29). For antigen retrieval, the slides were boiled in an autoclave in EDTA buffer (pH 8.0) for 10 min. The slides were incubated with the primary Skp2 antibody

at a dilution of 1:250 overnight at 4°C. The evaluation was done semiquantitatively. The cases with <5% positive tumor cells were scored as negative and tumors with >5% of positive tumor cells were evaluated as positive.

Statistics. To test the association of *MYCN in vitro* clusters with clinical and genetic data (overall survival, event-free survival, genomic *MYCN* status, and *E2F-1* gene expression), Global Test from the globaltest package of the R software package was used (Supplementary Methods; ref. 30). Because of multiple testing, Global Test *P* values were adjusted according to Benjamini and Yekutieli (31). Differential gene expression was evaluated for *MYCN* amplified versus all *MYCN* single-copy tumors, and also pairwise for all combinations of the following subgroups of *MYCN* single-copy tumors, stage 1, 2, 3/stage 4s/stage 4, using the Wilcoxon sum rank test. *P* values were adjusted using the Bonferroni-Holm procedure. Pearson's correlation was used to evaluate correlation among *MYCN*, *E2F-1*, and *Skp2* expression. To identify a model describing the relationship between survival and *Skp2* expression, the functional form of the relationship was tested by maximally selected log-rank statistics as previously described (25, 32). The resulting model was applied in further survival analyses. Multivariate Cox regression was used to investigate the prognostic power of candidate gene expression adjusting for established prognostic variables. To correct for overestimation of the hazard ratio estimate due to selection of the functional form of candidate gene expression variables, shrinkage of the variable estimate was applied (33). The Cox proportional hazards regression were done with the use of the design and survival package of the R software environment version 2.3.1.¹⁰ All reported *P* values are two sided.

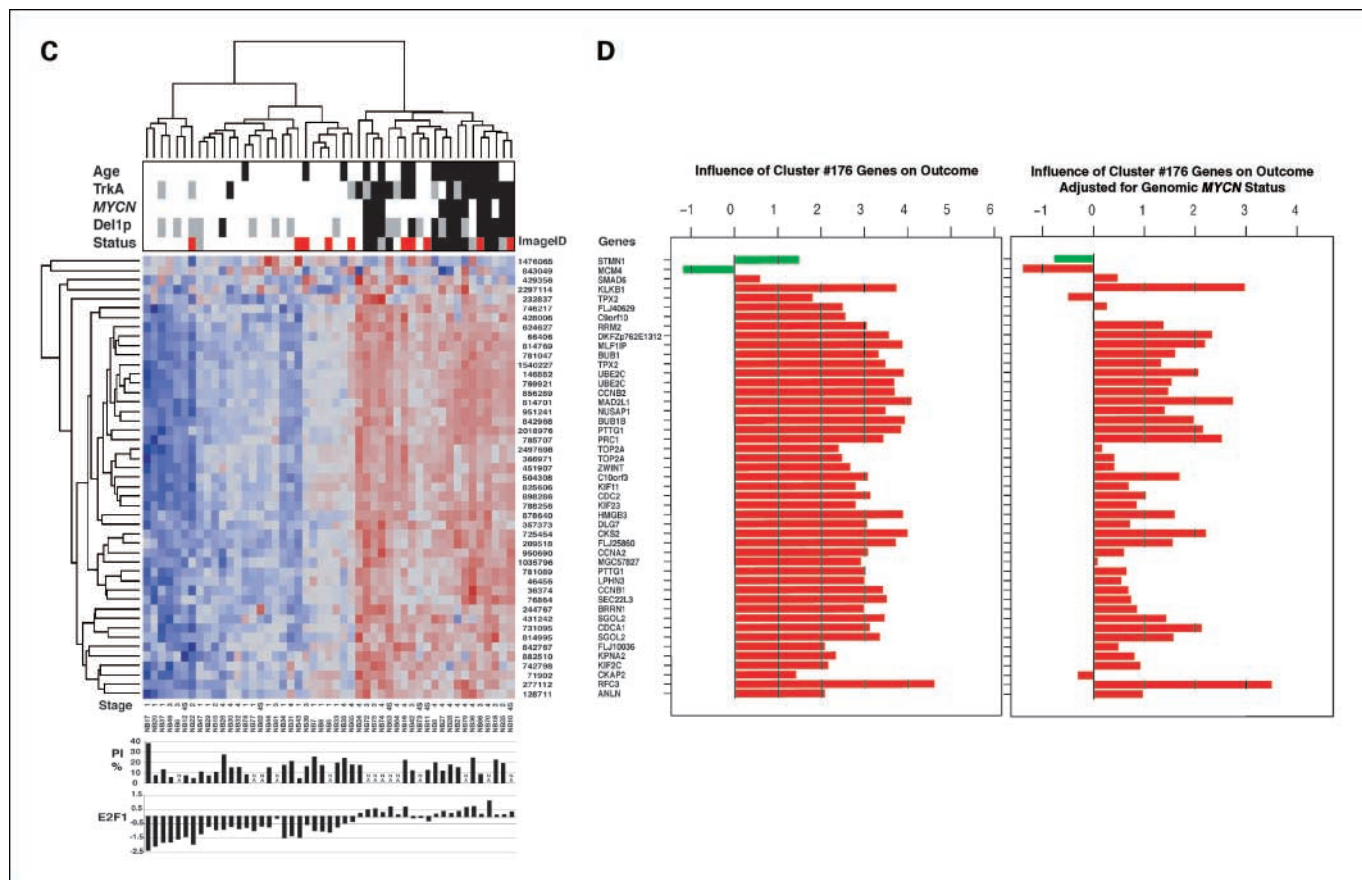


Fig. 1 Continued.

Results

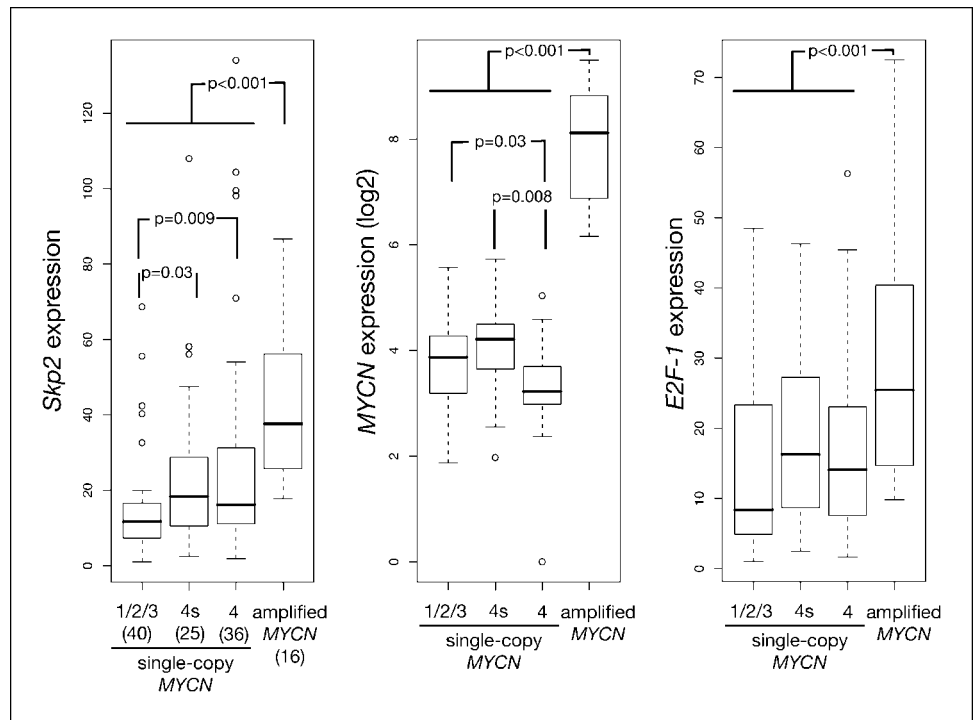
High expression of MYCN/MYC- and E2F-regulated genes identifies high-risk neuroblastomas independent of genomic MYCN status. To identify genetic programs associated with targeted MYCN expression *in vitro*, we made use of SH-EP-MYCN cells that express a MYCN transgene under the control of a tetracycline-repressible element in the human neuroblastoma cell line SH-EP (22). We collected total RNA from time course experiments after targeted MYCN expression at different experimental conditions and generated gene expression profiles using genome-wide cDNA microarrays. To better distinguish MYCN from E2F target genes, we inhibited E2F activity in a subset of experiments using low serum and low-dose doxorubicin, which left MYCN target gene activation largely unaffected (Supplementary Data and Methods). We combined these time course experiments and used self-organizing maps to capture the predominant patterns of gene expression. We applied a variance filter to select gene clusters that exhibited the most prominent transcriptional changes associated with targeted MYCN expression. By this procedure, 33 clusters were identified (Supplementary Fig. S1). As adjacent clusters within the cluster map showed similar gene expression profiles, the 33 clusters were further grouped into five cluster groups (A, B, C, D, and E).

We evaluated the expression of each of the 33 selected clusters in a set of 49 neuroblastoma tumors. For this, we used

the Global Test as proposed by Goeman et al. (30) and tested the association of each of the 33 *in vitro* clusters with overall survival and event-free survival directly, without the intermediary of single gene testing. We also tested the association of each of the 33 *in vitro* clusters with genomic MYCN status and E2F-1 expression in neuroblastoma tumors. Most *in vitro* clusters were significantly associated with poor outcome [overall survival (29 of 33, $P < 0.05$) and event-free survival (30 of 33, $P < 0.05$)] after adjusting the P values for multiple testing (Supplementary Table S1). Direct targets of MYCN/MYC transcription factors were enriched in group A clusters, as revealed by comparisons with the MYC target gene database¹² and the literature (34–36). Figure 1 shows a two-way hierarchical cluster analysis (A) and Global Test gene plots (B) using genes from a representative group A cluster, cluster 1, in which MYCN was arranged by the self-organizing map analysis. High MYCN expression showed a lower association with poor outcome (only >2 SD above the reference line 0) than other cluster 1 genes, including *Skp2*, *FLJ20485*, *MTHFD2*, *RG9MTD1*, *ILF2*, *SLC25A4*, *GMPS*, and *DKC1* (>4 SD above the reference line; Fig. 1B, left). Intriguingly, when the model was adjusted for genomic MYCN status, most of these genes remained significantly associated with poor outcome, whereas MYCN expression lost its association

¹² <http://www.mycncancergene.org>

Fig. 2. Expression of *Skp2*, *MYCN*, and *E2F-1* in 117 primary neuroblastomas as determined by QPCR. Data are represented as box plots: horizontal boundaries of the box represent the 25th and 75th percentile. The 50th percentile (median) is denoted by a horizontal line in the box and whiskers above and below extend to the most extreme data point which is no more than 1.5 times the interquartile range from the box. Differential gene expression was evaluated between *MYCN*-amplified versus all *MYCN* single-copy tumors, and pairwise for subgroups of *MYCN* single-copy tumors (stage 1, 2, 3/stage 4s/stage 4) using the Wilcoxon sum rank test. *P* values were adjusted using the Bonferroni-Holm procedure. Note that *MYCN* expression values were log₂ transformed to better visualize differences in *MYCN* single-copy neuroblastomas.



with poor outcome (Fig. 1B, right). *DKC1*, *SLC25A4*, and *MTHFD2* are directly regulated by MYC transcription factors, including c-MYC and/or MYCN (34–36). Additional genes directly regulated by MYC transcription factors were found in other group A clusters, such as *SFRS1*, *LARS*, and *ZNF146* (34–36), the high expression of which was also significantly associated with poor outcome independent of genomic MYCN status (data not shown). Group B clusters represent a genetic program predominantly comprising bona fide targets of E2Fs, such as *MAD2L1*, *CDC2*, *CCNA2*, *CCNB1/2*, *PTTG1*, and *CKS2* (13, 37, 38), from cluster 176 (Fig. 1C). In line with this, group B clusters were highly associated with *E2F-1* in neuroblastoma tumors (adjusted $P < 0.001$, Supplementary Table S1). High expression of group B cluster genes was also significantly associated with poor outcome independent of genomic MYCN status (Fig. 1D). Together, this revealed that a subset of MYCN and E2F targets are up-regulated in high-risk neuroblastoma tumors independent of genomic MYCN status and MYCN expression in MYCN single-copy tumors.

Expression of MYCN/MYC and E2F target genes does not correlate with proliferation activity in neuroblastoma tumors. To answer the question whether high expression of MYCN/MYC and E2F target genes simply reflects high proliferation activity, fluorescence-activated cell sorting cell cycle analyses of 4',6-diamidino-2-phenylindole-stained nuclei from the respective neuroblastoma specimens were done (31 of 49 specimens were available for this analysis). Intriguingly, tumor cell proliferation indices (%S phase + %G₂-M phase) were not higher in neuroblastomas with elevated expression of MYCN/MYC (Fig. 1A) and E2F targets (Fig. 1C). Further, favorable neuroblastomas with high proliferation indices (NB17, NB7, NB26) had low expression levels of MYCN/MYC and E2F targets. This is in line with fluorescence-activated cell sorting

cell cycle analyses in a large series of neuroblastoma specimens ($n = 143$) showing that high tumor cell proliferation indices were not associated with poor outcome in neuroblastoma tumors.¹³ Accordingly, high levels of a subset of MYCN/MYC- and E2F-regulated genes in high-risk neuroblastoma tumors were not merely due to increased proliferation of the corresponding tumor cells.

***Skp2* expression correlates positively with *E2F-1* and negatively with *p27* in neuroblastoma tumors.** Due to its central role in controlling both MYC and E2F functions, we further evaluated *Skp2* in relation to MYCN and *E2F-1* expression in a panel of 117 neuroblastomas by using specific quantitative reverse transcription-PCR. Relative expression values for *Skp2*, MYCN, and *E2F-1* expression were normalized to the geometric mean of *HPRT1* and *SDHA* expression values (24). *Skp2* mRNA levels correlated tightly with *E2F-1* mRNA levels as shown by QPCR [Pearson's correlation coefficient (PC) = 0.70; 95% confidence interval (95% CI), 0.60-0.79] and microarray analysis (PC = 0.84; 95% CI, 0.74-0.91). Even in the subset of MYCN single-copy tumors, *Skp2* mRNA levels correlated tightly with *E2F-1* mRNA levels [PC = 0.69; 95% CI, 0.57-0.78 (QPCR); PC = 0.8; 95% CI, 0.64-0.89 (microarray)]. This is in line with the proposed regulation of *Skp2* by Rb-E2F (39). Expression of *Skp2* was significantly higher in MYCN-amplified tumors than in MYCN single-copy tumors ($P < 0.001$; Fig. 2). However, *Skp2* expression was poorly associated with MYCN expression in MYCN single-copy tumors [PC = 0.24; 95% CI, 0.03-0.44 (QPCR), PC = 0.21; 95% CI, -0.12-0.50 (microarray)]. In the subset of MYCN single-copy tumors, we found that *Skp2* mRNA levels were significantly higher in stage 4 ($P = 0.009$) and 4s tumors ($P = 0.03$) than in

¹³ Unpublished data.

localized (stage 1, 2, 3) tumors. Remarkably, whereas *Skp2* mRNA levels were not different in stage IVs versus stage IV tumors ($P = 0.92$), *MYCN* mRNA levels were significantly higher in stage IVs than in stage IV *MYCN* single-copy tumors ($P = 0.008$). The primary target of the SCF^{Skp2} ubiquitin ligase during cell cycle progression is the p27 protein, the expression of which is reduced in high-risk neuroblastomas (40). We investigated p27 and Skp2 protein expression using a paraffin multitissue array consisting of 141 neuroblastoma tumor specimens. Probably due to antigen masking, the detection limit for both proteins was high. We did not detect either of both proteins in 113 tumor samples. In 28 samples, we detected a mutually exclusive expression of Skp2 [$n = 16$; amplified = 7, stage 4 single-copy (sc) = 3, stage 3 sc = 2, stage 1/2 sc = 4] and p27 ($n = 12$; amplified = 1, stage 4 sc = 2, stage 3 sc = 2, stage 1/2/4s sc = 7) protein. In line with our QPCR analysis, strongest Skp2 protein staining was observed in *MYCN*-amplified tumors (Fig. 3A). We also did more sensitive immunoblotting for Skp2 and p27 in neuroblastoma tumors. Detection of Skp2 protein was associated with reduced p27 protein levels in neuroblastoma tumors (Fig. 3B).

Skp2 expression correlates with poor outcome in neuroblastoma patients independent of genomic *MYCN* status. The search for a model describing the relationship between survival and *Skp2* gene expression using maximally selected log-rank statistics identified a cut point model to be most suitable: A *Skp2* QPCR cutoff value of 25.7 separated two patient subgroups with significantly different outcome [maximally selected log-rank statistics, $P < 0.001$ (event-free survival), $P = 0.002$ (overall survival)]. Applying this *Skp2* expression cutoff to Kaplan-Meier survival curve estimation revealed increased recurrence rate and decreased survival probability for patients with tumor expressing high levels of *Skp2* (Fig. 4). As *Skp2* is induced by targeted *MYCN* expression *in vitro* and its expression is significantly correlated with amplified *MYCN*, we asked whether *Skp2* expression adds prognostic information independent of *MYCN* status. High *Skp2* was associated with increased recurrence rate ($P = 0.001$) and decreased survival probability ($P = 0.02$) also in *MYCN* single-copy neuroblastomas (Fig. 4). To determine whether *Skp2* expression provides additional predictive power over other established prognostic markers, multivariate survival analysis was done. The risk factors included in the model were all associated with decreased event-free survival in univariate analysis: amplified *MYCN* ($P = 0.005$), stage 4 ($P < 0.001$), and age at diagnosis >1.5 years ($P < 0.001$). Cox proportional hazards models were built based on 117 patients. Together with age at diagnosis >1.5 years, high *Skp2* expression was selected as a statistically significant predictor for decreased event-free survival (Table 2). To further illustrate the prognostic independence of *Skp2* expression from amplified *MYCN*, multivariate survival analysis was done in the subgroup of 101 tumors with single-copy *MYCN*. *Skp2* expression, together with age at diagnosis >1.5 years, emerged as independent factor even in this cohort (Table 3).

Discussion

In this study, we found that transcript profiling of a neuroblastoma *in vitro* system that allows conditional expression of *MYCN* delineates *MYCN* downstream genetic programs

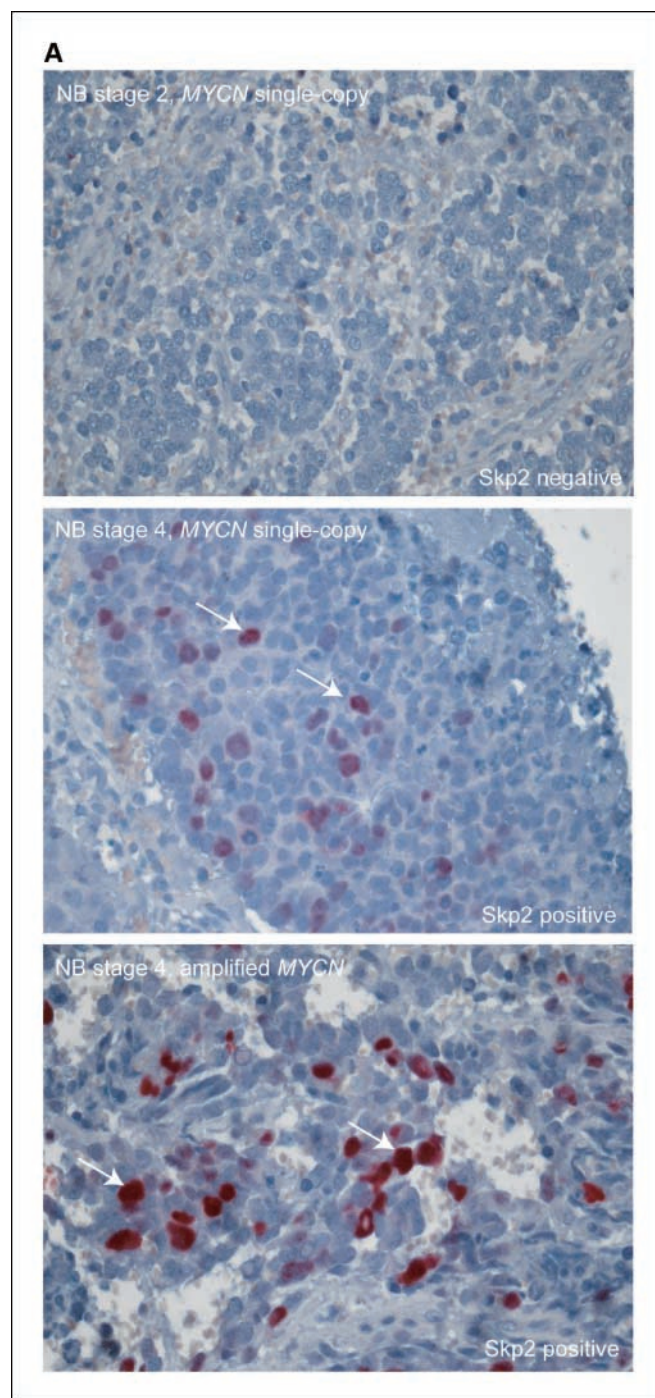
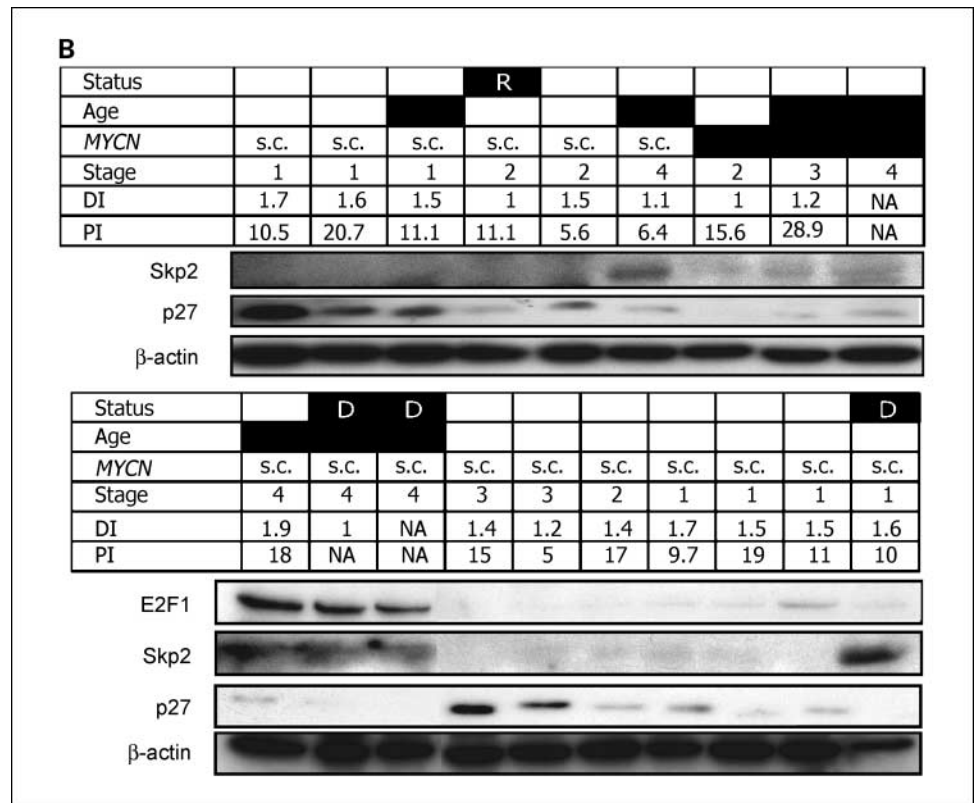


Fig. 3. Skp2 protein expression in neuroblastoma specimens. A, immunohistochemistry.

that are associated with patients' outcome independent of genomic *MYCN* status. The identified *MYCN* downstream genetic programs consisted of direct targets of MYC transcription factors (group A clusters, e.g., cluster 1), and of direct E2F targets (group B clusters, e.g., cluster 176). For *MYCN* single-copy tumors with poor outcome, high expression of *MYCN*/*MYC* target genes was unexpected, because *MYCN* mRNA and protein levels are usually lower in these tumors than in favorable *MYCN* single-copy tumors, as shown by results from

Fig. 3 Continued. B. Western blot analysis. β -Actin was used as a loading control. Age, ■ ≥ 1.5 y at diagnosis, MYCN, ■, amplified MYCN. DI, DNA index; PI, proliferation index (%S phase + %G₂-M phase); R, relapse/progression; D, death due to neuroblastoma; s.c., MYCN single-copy.



independent studies (6, 7) and those presented here. In addition, expression of other MYC transcription factors is not associated with poor outcome in MYCN single-copy tumors.¹³ As an alternative mechanism for MYCN target gene activation in MYCN single-copy neuroblastoma tumors, we considered the deregulated activity of a cofactor involved in transcriptional activation by MYC proteins, namely Skp2, the F-box protein of the SCF^{Skp2} E3 ligase.

High *Skp2* mRNA levels strongly correlated with amplified MYCN and poor outcome as measured by cDNA microarray ($n = 49$) and QPCR ($n = 117$) in two primary neuroblastoma tumor cohorts. Notably, our multivariate survival analysis for event-free survival identified "Skp2 expression" as a predictor variable that was independent not only of the variable "amplified MYCN" but also of "stage" (stage 4 versus stage 1, 2, 2, and 4s). The prognostic independence of *Skp2* expression from amplified MYCN was further shown by multivariate survival analysis within the subgroup of MYCN single-copy neuroblastomas ($n = 101$). This indicates that high *Skp2* expression is a shared feature of MYCN-amplified and single-copy high-risk neuroblastomas.

We found that high Skp2 correlated with low p27 protein levels, the primary target of the SCF^{Skp2} E3-ligase, in primary neuroblastoma tumors. This is in line with results from other cancer types that showed a correlation of high Skp2 with low p27 protein levels and advanced grade of malignancy (41). The association of low p27 protein levels with poor outcome in primary neuroblastoma tumors was described earlier (40); however, a link to deregulated Skp2 was not yet established. Our microarray and QPCR data further revealed the transcriptional changes associated with high *Skp2* expression in

neuroblastoma tumors: Expression of *Skp2* is tightly correlated with *E2F-1* and E2F activity. This is in line with previous *in vitro* results that established *Skp2* as a direct E2F-1 target (42). Additionally, Skp2 also strongly influences E2F functions. First, Skp2 favors the degradation of p27 and p21 during G₁-S phase transition leading to cyclin-dependent kinase activation that mediates the release of E2F family proteins via Rb phosphorylation (17, 41). Second, Skp2 is required for G₂-M progression via mediating the degradation of p27, newly synthesized during S-phase progression (18). In line with these proposed Skp2 functions, we found that high *Skp2* is associated with high expression of E2F targets encoding G₂-M activities [*MAD2L1*, *CDC2*, *CCNB1/2*, *PTTG1* (cluster 176)] in high-risk neuroblastomas that often fail to express p27. Importantly, high expression of these E2F targets did not merely reflect elevated proliferation of the respective tumor cells, because expression of these E2F target genes did not correlate with tumor cell proliferation as determined by fluorescence-activated cell sorting cell cycle analysis.

It has been described that Skp2 also acts as cofactor for c-MYC-dependent transcriptional activation independent of its proteolytic function (15). Thus far, it is unclear whether high Skp2 also influences MYCN activity in neuroblastoma cells. We observed that MYCN/MYC targets genes (group A clusters, e.g., cluster 1), including *DKC1*, *SLC25A4*, *MTHFD2*, strongly correlated with *Skp2* in neuroblastoma tumors. It is tempting to speculate that high Skp2 activity does not only favor transcriptional activation in MYCN-amplified neuroblastomas, but also in high-risk MYCN single-copy neuroblastomas even in the absence of high levels of MYCN or other MYC proteins.

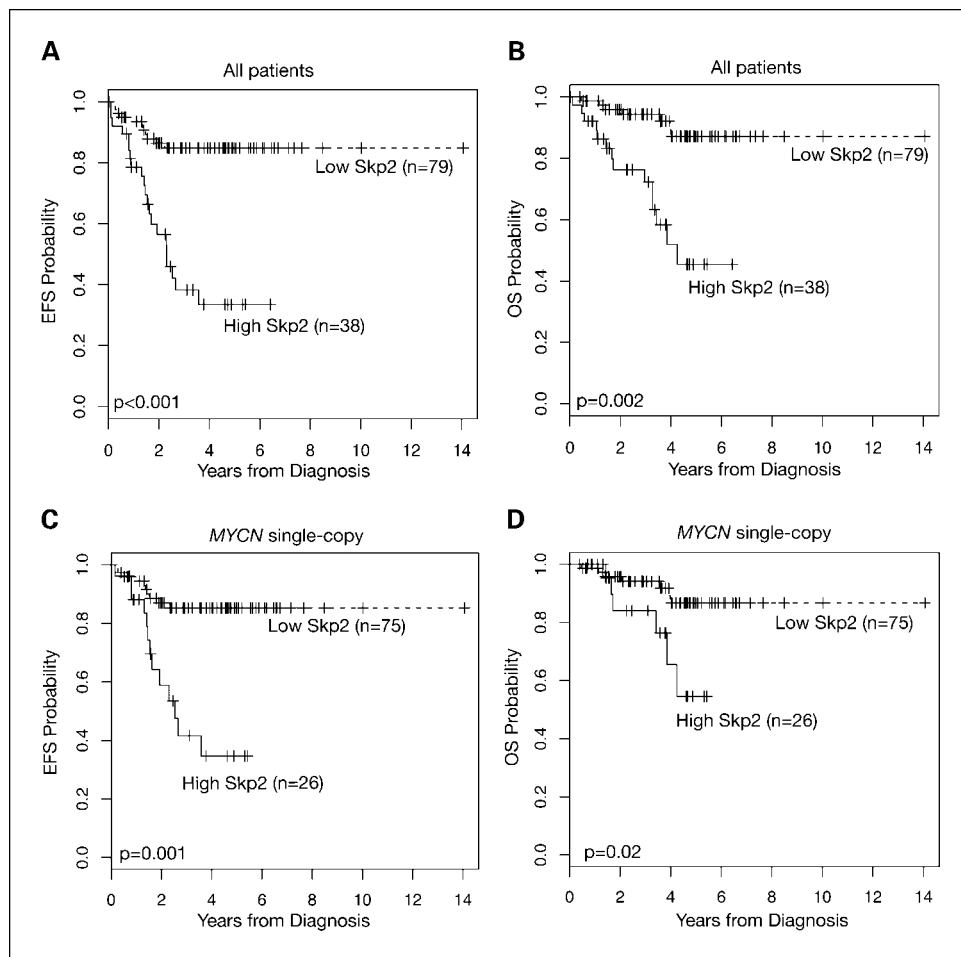


Fig. 4. Kaplan-Meier estimates of event-free survival (EFS) and overall survival (OS) in relation to *Skp2* expression as determined by QPCR. Kaplan-Meier estimates are given for all patients (A and B) and the subgroup of *MYCN* single-copy neuroblastomas (C and D). Cutoff value for dichotomization of *Skp2* expression and *P* values were determined by maximally selected log-rank statistics. High *Skp2*, QPCR >25.7; low *Skp2*, QPCR ≤25.7.

An unexpected finding in this study was that mRNA levels of *Skp2* and *E2F-1* were not significantly different in *MYCN* single-copy stage 4 versus stage 4s neuroblastomas, two neuroblastoma subtypes with contrasting clinical outcome. It was observed that p27 protein levels are significantly lower in stage 4 than in stage 4s *MYCN* single-copy tumors (40). This argues in favor of a higher activity of the SCF^{Skp2} E3-ligase in stage 4 than in

stage 4s. Therefore, we suggest that Skp2 activity is differentially controlled via transcriptional independent mechanisms in these tumors. Skp2 activity is strongly inhibited via a direct interaction with the Rb protein (43). Intriguingly, this Rb function is independent of its E2F controlling function. Future studies should address the regulation of Skp2 in different neuroblastoma subtypes at the protein level.

Table 2. Cox proportional hazards regression for event-free survival (n = 117, QPCR cohort)

Variable	Effect	Hazard ratio (95% CI)	P
<i>Skp2</i> expression*	High vs low	3.54 (1.56-8.00)	0.002
Age at diagnosis (y)	≥1.5 vs <1.5	2.86 (1.06-7.70)	0.04
Disease stage	4 vs 1, 2, 3, 4s	1.68 (0.62-4.52)	0.30
<i>MYCN</i> amplification	Yes vs no	1.17 (0.52-2.61)	0.71

*The cutoff value for dichotomization of *Skp2* expression was estimated by maximally selected log-rank statistics. A corrected estimated hazard ratio is given after application of a shrinkage procedure to correct for bias, together with bootstrap resampling using 1,000 bootstrap samples for estimating the variance (33).

Table 3. Cox proportional hazards regression for event-free survival without *MYCN* amplification (n = 101, QPCR cohort)

Variable	Effect	Hazard ratio (95% CI)	P
<i>Skp2</i> expression*	High vs low	3.21 (1.02-10.11)	0.05
Age at diagnosis (y)	≥1.5 vs <1.5	4.87 (1.39-17.11)	0.01
Disease stage	4 vs 1, 2, 3, 4s	1.29 (0.37-4.51)	0.69

*The cutoff value for dichotomization of *Skp2* expression was estimated by maximally selected log-rank statistics. A corrected estimated hazard ratio is given after application of a shrinkage procedure to correct for bias, together with bootstrap resampling using 1,000 bootstrap samples for estimating the variance (33).

In summary, our data suggest that Skp2 is an important player in the development and progression of neuroblastomas, and may consequently be an attractive target for therapeutic approaches including proteasome inhibitors and/or differentiation-inducing agents that suppress SCF^{Skp2} E3 ligase activity.

Acknowledgments

We thank Steffen Bannert, Marc Matuszewski, Jochen Kreth, Jana Faut, Heike Düren, and Yvonne Kahlert for technical assistance; Frank Berthold, Barbara Hero, André Oberthür, and the German neuroblastoma Study Group for providing neuroblastoma tumor samples and clinical data; and Rüdiger Spitz for providing 1p fluorescence *in situ* hybridization data.

References

- Schwab M, Westermann F, Hero B, Berthold F. Neuroblastoma: biology and molecular and chromosomal pathology. *Lancet Oncol* 2003;4:472–80.
- Brodeur GM. Neuroblastoma: biological insights into a clinical enigma. *Nat Rev* 2003;3:203–16.
- Brodeur GM, Seeger RC, Schwab M, Varmus HE, Bishop JM. Amplification of N-myc in untreated human neuroblastomas correlates with advanced disease stage. *Science* 1984;224:1121–4.
- Weiss WA, Aldape K, Mohapatra G, Feuerstein BG, Bishop JM. Targeted expression of MYCN causes neuroblastoma in transgenic mice. *EMBO J* 1997;16:2985–95.
- Schwab M, Varmus HE, Bishop JM. Human N-myc gene contributes to neoplastic transformation of mammalian cells in culture. *Nature* 1985;316:160–2.
- Cohn SL, London WB, Huang D, et al. MYCN expression is not prognostic of adverse outcome in advanced-stage neuroblastoma with nonamplified MYCN. *J Clin Oncol* 2000;18:3604–13.
- Tang XX, Zhao H, Kung B, et al. The MYCN enigma: significance of MYCN expression in neuroblastoma. *Cancer Res* 2006;66:2826–33.
- Ohira M, Oba S, Nakamura Y, et al. Expression profiling using a tumor-specific cDNA microarray predicts the prognosis of intermediate risk neuroblastomas. *Cancer Cell* 2005;7:337–50.
- Berwanger B, Hartmann O, Bergmann E, et al. Loss of a FYN-regulated differentiation and growth arrest pathway in advanced stage neuroblastoma. *Cancer Cell* 2002;2:377–86.
- Wei JS, Greer BT, Westermann F, et al. Prediction of clinical outcome using gene expression profiling and artificial neural networks for patients with neuroblastoma. *Cancer Res* 2004;64:6883–91.
- Krasnoselsky AL, Whiteford CC, Wei JS, et al. Altered expression of cell cycle genes distinguishes aggressive neuroblastoma. *Oncogene* 2005;24:1533–41.
- Alaminos M, Mora J, Cheung NK, et al. Genome-wide analysis of gene expression associated with MYCN in human neuroblastoma. *Cancer Res* 2003;63:4538–46.
- Hernando E, Nahle Z, Juan G, et al. Rb inactivation promotes genomic instability by uncoupling cell cycle progression from mitotic control. *Nature* 2004;430:797–802.
- Huang E, Ishida S, Pittman J, et al. Gene expression phenotypic models that predict the activity of oncogenic pathways. *Nat Genet* 2003;34:226–30.
- von der Lehr N, Johansson S, Wu S, et al. The F-box protein Skp2 participates in c-Myc proteasomal degradation and acts as a cofactor for c-Myc-regulated transcription. *Mol Cell* 2003;11:1189–200.
- Carrano AC, Eytan E, Hershko A, Pagano M. SKP2 is required for ubiquitin-mediated degradation of the CDK inhibitor p27. *Nat Cell Biol* 1999;1:193–9.
- Bornstein G, Bloom J, Sitry-Shevah D, Nakayama K, Pagano M, Hershko A. Role of the SCF^{Skp2} ubiquitin ligase in the degradation of p21Cip1 in S phase. *J Biol Chem* 2003;278:25752–7.
- Nakayama K, Nagahama H, Minamishima YA, et al. Skp2-mediated degradation of p27 regulates progression into mitosis. *Dev Cell* 2004;6:661–72.
- London WB, Boni L, Simon T, et al. The role of age in neuroblastoma risk stratification: the German, Italian, and Children's Oncology Group perspectives. *Cancer Lett* 2005;228:257–66.
- Berthold F, Sahin K, Hero B, et al. The current contribution of molecular factors to risk estimation in neuroblastoma patients. *Eur J Cancer* 1997;33:2092–7.
- Huber W, von Heydebreck A, Sultmann H, Poustka A, Vingron M. Variance stabilization applied to microarray data calibration and to the quantification of differential expression. *Bioinformatics* 2002;18 Suppl 1: S96–104.
- Lutz W, Stohr M, Schurmann J, Wenzel A, Lohr A, Schwab M. Conditional expression of N-myc in human neuroblastoma cells increases expression of α -prothymosin and ornithine decarboxylase and accelerates progression into S-phase early after mitogenic stimulation of quiescent cells. *Oncogene* 1996;13:803–12.
- Fulda S, Lutz W, Schwab M, Debatin KM. MycN sensitizes neuroblastoma cells for drug-induced apoptosis. *Oncogene* 1999;18:1479–86.
- Fischer M, Skowron M, Berthold F. Reliable transcript quantification by real-time reverse transcriptase-polymerase chain reaction in primary neuroblastoma using normalization to averaged expression levels of the control genes HPRT1 and SDHA. *J Mol Diagn* 2005;7:89–96.
- Henrich KO, Fischer M, Mertens D, et al. Reduced expression of CAMTA1 correlates with adverse outcome in neuroblastoma patients. *Clin Cancer Res* 2006;12:131–8.
- Ehemann V, Hashemi B, Lange A, Otto HF. Flow cytometric DNA analysis and chromosomal aberrations in malignant glioblastomas. *Cancer Lett* 1999;138:101–6.
- Wiedemeyer R, Westermann F, Wittke I, Nowock J, Schwab M. Ataxin-2 promotes apoptosis of human neuroblastoma cells. *Oncogene* 2003;22:401–11.
- Hell K, Lorenzen J, Hansmann ML, Fellbaum C, Busch R, Fischer R. Expression of the proliferating cell nuclear antigen in the different types of Hodgkin's disease. *Am J Clin Pathol* 1993;99:598–603.
- Baldus SE, Schneider PM, Monig SP, et al. p21/waf1/cip1 in gastric cancer: associations with histopathological subtypes, lymphonodal metastasis, prognosis and p53 status. *Scand J Gastroenterol* 2001;36:975–80.
- Goeman JJ, Oosting J, Cleton-Jansen AM, Anninga JK, van Houwelingen HC. Testing association of a pathway with survival using gene expression data. *Bioinformatics* 2005;21:1950–7.
- Benjamini Y, Yekutieli D. The control of the false discovery rate in multiple testing under dependency. *Ann Stat* 2001;29:1165–88.
- Lausen B, Schumacher M. Maximally selected rank statistics. *Biometrics* 1992;48:73–85.
- Hollander N, Sauerbrei W, Schumacher M. Confidence intervals for the effect of a prognostic factor after selection of an "optimal" cutpoint. *Stat Med* 2004;23:1701–13.
- Guo QM, Malek RL, Kim S, et al. Identification of c-myc responsive genes using rat cDNA microarray. *Cancer Res* 2000;60:5922–8.
- Fernandez PC, Frank SR, Wang L, et al. Genomic targets of the human c-Myc protein. *Genes Dev* 2003;17:1115–29.
- Boon K, Caron HN, van Asperen R, et al. N-myc enhances the expression of a large set of genes functioning in ribosome biogenesis and protein synthesis. *EMBO J* 2001;20:1383–93.
- Zhu W, Giangrande PH, Nevins JR. E2Fs link the control of G₁/S and G₂/M transcription. *EMBO J* 2004;23:4615–26.
- Ren B, Cam H, Takahashi Y, et al. E2F integrates cell cycle progression with DNA repair, replication, and G(2)/M checkpoints. *Genes Dev* 2002;16:245–56.
- Vernell R, Helin K, Muller H. Identification of target genes of the p16INK4A-pRB-E2F pathway. *J Biol Chem* 2003;278:46124–37.
- Bergmann E, Wanzel M, Weber A, Shin I, Christiansen H, Eilers M. Expression of P27 (KIP1) is prognostic and independent of MYCN amplification in human neuroblastoma. *Int J Cancer* 2001;95:176–83.
- Bloom J, Pagano M. Deregulated degradation of the cdk inhibitor p27 and malignant transformation. *Semin Cancer Biol* 2003;13:41–7.
- Zhang L, Wang C. F-box protein Skp2: a novel transcriptional target of E2F. *Oncogene* 2006;25:2615–27.
- Ji P, Jiang H, Reikhtman K, et al. An Rb-Skp2-27 pathway mediates acute cell cycle inhibition by Rb and is retained in a partial-penetrance Rb mutant. *Mol Cell* 2004;16:47–58.